SCIENTIFIC REPORTS
nature research

OPEN

Photosystem II of *Ligustrum lucidum* in response to different levels of manganese exposure

Received: 20 March 2018
Accepted: 31 July 2019
Published online: 29 August 2019

Hui-Zi Liang[1], Fan Zhu[1,2], Ren-Jie Wang[2], Xin-Hao Huang[1] & Jing-Jing Chu[1]

The toxic effect of excessive manganese (Mn) on photosystem II (PSII) of woody species remains largely unexplored. In this study, five Mn concentrations (0, 12, 24, 36, and 48 mM) were used, and the toxicity of Mn on PSII behavior in leaves of *Ligustrum lucidum* was investigated using *in vivo* chlorophyll fluorescence transients. Results showed that excessive Mn levels induced positive L- and K- bands. Variable fluorescence at 2 ms (V_J) and 30 ms (V_I), absorption flux (ABS/RC), trapped energy flux (TR_o/RC), and dissipated energy flux (DI_o/RC) increased in Mn-treated leaves, whereas the performance index (PI_{ABS}), electron transport flux (ET_o/RC), maximum quantum yield (φ_{Po}), quantum yield of electron transport (φ_{Eo}), and probability that an electron moves further than Q_A^- (ψ_o) decreased. Also, excessive Mn significantly decreased the net photosynthesis rate and increased intercellular CO_2 concentration. The results indicated that Mn blocked the electron transfer from the donor side to the acceptor side in PSII, which might be associated with the accumulation of Q_A^-, hence limiting the net photosynthetic rate.

It is well-known that manganese (Mn) is an essential micronutrient element required for the growth and development of plants. Especially, Mn is involved in metabolic pathways of chlorophyll (Chl) synthesis and breakdown in the chloroplasts[1,2]. The oxygen-evolving complex (OEC) of photosystem II (PSII) contains a Mn-containing metalloenzyme core. This inorganic core, binding to the reaction center (RC) protein D1 in PSII, has the empirical formula Mn_4CaO_5 and is known as the tetra-nuclear Mn cluster[3,4]. However, Mn, in excess, is also considered as one of the most toxic trace metals to plants. Mn pollution often originates from industrial disposal[5], manufacturing sewage[6,7], as well as mineral exploitation[8].

Toxic effects of Mn on plants is well documented. Excessive Mn level impedes plant growth and development by interfering with metabolic processes[9,10]. Moreover, a number of studies have shown that Mn mainly exerts its toxicity to plant leaves by inhibiting photosynthesis and chloroplast activity[9–12] leading to reduced chloroplast content and suppressed CO_2 assimilation[13–16]. PSII is highly sensitive to Mn level. Feng *et al.*[13] have reported that excessive Mn inhibits the maximum photochemical efficiency (F_v/F_M) and effective quantum yield of PSII (ΦPSII) in cucumber. Doncheva *et al.*[17] have shown that excessive Mn significantly affects the quantum efficiency of PSII in Mn-sensitive maize (*Zea mays L.*) 'Kneja 605', but not in Mn-tolerant maize 'Kneja 434'. Interestingly, some other studies have revealed that F_v/F_M is not substantially affected by Mn accumulation in tobacco and rice bean seedlings[11,18]. In addition, Kitao *et al.*[19] have suggested that excessive Mn affects the activity of CO_2 reduction cycle rather than F_v/F_M in white birch, while increased Q_A reduction and thermal energy dissipation, as well as decreased quantum yield of PSII, have been observed. Similar results have been found in *Alnus hirsuta* Turcz., *Betula ermanii* Cham., *Ulmus davidiana* Planch., and *Acer mono* Maxim[15]. Li *et al.*[16] have reported that excessive Mn impairs the whole photosynthetic electron transport chain from the donor side of PSII up to the reduction of end acceptors of PSI in *Citrus grandis* seedlings, followed by the increase in ABS/RC, TR_o/RC, and DI_o/RC, as well as decrease in ET_o/RC, φ_{Po}, and ψ_o. However, the mechanism of toxicity of Mn to PSII remains largely unexplored, and most previous studies have only focused on herbaceous plants[11,13,17,18].

Chl a fluorescence, a non-invasive spectroscopic technique, has been widely used to detect and measure the *in vivo* behavior of PSII under different environmental stresses[20,21]. Analysis of the polyphasic fluorescence transient under physiological conditions shows that the fluorescence increases in the typical shape of OJIP kinetics[21].

[1]College of Life Science and Technology, Central South University of Forestry and Technology, Changsha, 410004, P. R. China. [2]Engineering Laboratory of Applied Technology for Forestry & Ecology in Southern China, Changsha, 410004, Hunan, China. Correspondence and requests for materials should be addressed to F.Z. (email: csuftzf@163.com)

The "JIP-test" analysis of the OJIP transients allows the calculation of structural, conformational, and functional parameters quantifying the PSII behavior under environmental stresses, including absorption flux, trapped energy flux, electron transport flux, and dissipated energy flux[21].

Hunan Province in the southern area of China has a high density of Mn mines. Severe pollution in agricultural lands, stream water, sediments, and soils have been reported in this area, threatening human health[8]. As an important evergreen broad-leaved tree species in the southern regions of China, *Ligustrum lucidum* is highly tolerant to heavy metals[22,23]. In this study, we aimed to investigate changes in the OJIP transient and related parameters in the leaves of *L. lucidum* in the presence of Mn. In addition, we evaluated the toxicity of Mn to PSII behavior when *L. lucidum* was cultured under Mn stress for up to 40 days.

Materials and Methods

Plant culture and Mn treatments. Two-year-old *L. lucidum* seedlings (average diameter, ~9 mm; height, ~133 cm) were purchased from a local nursery. All plants were individually transplanted into plastic pots (diameter, 25.4 cm; height, 17.8 cm) filled with 7 kg of air-dried soil. The plants were grown under natural illumination (30/25 °C day/night temperature, 12/12 h day/night cycle and a maximum photosynthetically active radiation of about 1,000 μmol photons m^{-2} s^{-1}) for 4 months to acclimatize them to the soil microclimate before initiating Mn treatment. Each pot was supplied with 400 mL of pure water every 2 to 3 days.

Samples of soil free from heavy metal pollution were collected from the CSUFT campus soil at a depth of 5–20 cm. The soil samples were taken back to the laboratory, and were sieved through 5 × 5 mm sieves to remove rocks, and were then air-dried at room temperature. The chemical properties of soil samples were as measured: pH 4.9, 0.227 g N/kg, 0.129 g P/kg, and 355.978 mg Mn/kg.

For the Mn-treated soil, distilled water containing 1.2 mM, 2.4 mM, 3.6 mM and 4.8 mM Mn from $MnCl_2{\cdot}5H_2O$ was added to the pots every other day at a rate of 400 mL per day for 20 days. The four Mn treatments were designated as L1, L2, L3, and L4, respectively. For the control (CK), about 400 mL of distilled water without Mn was added into the pots. In total we have five treatments: CK, L1, L2, L3 and L4, and each treatment was replicated five times. Measurements were carried out on three fully expanded *L. lucidum* leaves of similar size on days 10, 25, and 40 after the Mn treatment.

Fast Chl a fluorescence kinetics and JIP-test. Fast Chl a fluorescence was measured by M-PEA (Multifunctional Plant Efficiency Analyzer, Hansatech Instrument, UK). Leaves were exposed to a pulse of saturating red light (5,000 μmol m^{-2} s^{-1}, peak 625 nm, duration 50 μs–2 s, records of 128 points) and measured daily between 8:30–11:00 am after 1 h of dark adaptation using dark adaptation clips. The fluorescence transients (OJIP curves) were analyzed to determine energy distribution through PSII per RC (ABS/RC, TR_o/RC, ET_o/RC, DI_o/RC, see Table 1), flux ratios (φ_{Po}, φ_{Eo}, and ψ_o) and performance index (PI_{ABS}) according to the JIP-test[19]. Relative variable fluorescence at time t, at the J-step, and at the I-step (i.e., V_t, V_J and V_I, respectively) was calculated using the following equations[16,21]:

$$V_t = (F_t - F_o)/(F_M - F_o) \quad (1)$$

$$V_J = (F_J - F_o)/(F_M - F_o) \quad (2)$$

$$V_I = (F_I - F_o)/(F_M - F_o) \quad (3)$$

$$\Delta V_t = V_t - V_{t(control)} \quad (4)$$

where F_J is fluorescence intensity at 2 ms and F_I is the fluorescence intensity at 30 ms.

To further characterize the effect of Mn on *L. lucidum* PSII, some functional parameters were calculated from the JIP-test. The OJIP transients were double normalized between O (50 μs) and P steps to estimate relative variable fluorescence $W_{OP} = (F_t - F_o)/(F_P - F_o)$. Normalization between O and K (300 μs) steps revealed L-band (150 μs), resulting in the variable fluorescence[24]:

$$W_{OK} = (F_t - F_o)/(F_K - F_o) \quad (5)$$

$$W_{OK(control)} = (F_t - F_o)/(F_K - F_o) \quad (6)$$

$$\Delta W_{OK} = W_{OK} - (W_{OK})_{control} \quad (7)$$

Normalization between O and J (2 ms) steps revealed K-band (300 μs), resulting in the variable fluorescence[24]:

$$W_{OJ} = (F_t - F_o)/(F_J - F_o) \quad (8)$$

$$\Delta W_{OJ} = W_{OJ} - (W_{OJ})_{control} \quad (9)$$

The F_I, F_J, F_K, F_M, and F_O represent fluorescence at I-step, J-step, and K-step, dark-adapted maximum fluorescence, and dark-adapted minimum fluorescence, respectively. ΔV_J, ΔV_I, ΔW_{OK}, and ΔW_{OJ} represent the J-band, I-band, L-band, and K-band, respectively, and are associated with the accumulation of Q_A^-[21], the proportion of

Data extracted from the recorded fluorescence transient OJIP	
$F_o \cong F_{50\mu s}$	Minimal fluorescence, when all RCs are open
$F_{300\mu s}$, F_{2ms}, F_{30ms}	Fluorescence intensity at 300 μs, 2 ms, 30 ms, respectively
FPs derived from the extracted data	
$V_t = (F_t - F_o)/(F_M - F_o)$	Relative variable fluorescence at time t
$V_J = (F_{2ms} - F_o)/(F_M - F_o)$	Relative variable fluorescence at the J-step (2 ms), reflects the activity of acceptor side of PSII
$V_I = (F_{30ms} - F_o)/(F_M - F_o)$	Relative variable fluorescence at the I-step (30 ms), reflects the activity of acceptor side of PSII
Specific energy fluxes (per Q_A reducing PSII RC)	
ABS/RC	Absorption flux (of antenna Chls) per RC (also a measure of PSII apparent antenna size)
TR_o/RC	Trapped energy flux (leading to Q_A reduction) per RC at t = 0
ET_o/RC	Electron transport flux (further than Q_A^-) per RC at t = 0
DI_o/RC	Dissipated energy flux per RC at t = 0
Quantum yields and efficiencies/probabilities	
$\varphi_{Po} = TR_o/ABS$	Maximum quantum yield for primary photochemistry
$\varphi_{Eo} = ET_o/ABS$	Quantum yield for electron transport
$\Psi_o = ET_o/TR_o$	Efficiency/probability that an electron moves further than Q_A^-
Performance index	
$PI_{ABS} = (RC/ABS)$ $(\varphi_{Po}/1 - \varphi_{Po}))(\psi_o/(1 - \psi_o))$	Performance index (potential) for energy conservation from photons absorbed by PSII to the reduction of intersystem electron acceptors

Table 1. Definition of terms and formulae of the selected JIP-test parameters.

Q_B-non-reducing PSII RCs[16], energetic connectivity of antennae to PSII RC units[24], and the activity of OEC of PSII donor side[25], respectively.

Gas exchange. Net photosynthetic rate (Pn) and intercellular CO_2 concentration (Ci) were measured by LI-COR 6400 portable photosynthesis system (LI-COR Bioscience, Lincoln, NE, USA). Measurements were carried out on three leaves per plant on day 40 with 1,000 μmol photon m^{-2} s^{-1}, and a 2 min measurement duration per sample.

Determination of total Mn content. The dried biomass of different organs (roots, stems, and leaves) was powdered and used to digested with 15 mL acid mixture ($HClO_4/HNO_3 = 1/4$). The concentration of Mn was determined by ICP-AES (Optima 8300, American platinum Elmer, USA).

Data analysis. Data were reported as means of each group based on at least six independent replicates. Results are presented as means ± standard error (SE). Statistical differences between measurements were analyzed using one-way ANOVA, followed by a least significant difference (LSD) test at $P < 0.05$. Chl a fluorescence parameters (FPs) associated with Mn levels and stress time were assessed using two-way ANOVA with $\alpha = 0.05$. All graphs were made using Sigmaplot 12.0.

Results

Effects of Mn on Chl a fluorescence transient and related parameters in *L. lucidum* leaves. All OJIP transients from both Mn-treated and control leaves showed a typical polyphasic rise with the basic steps of O-J-I-P. Mn-treated leaves displayed positive trends of K-, J-, and I-bands compared with the controls at 300 μs, 2 ms, and 30 ms, respectively (Fig. 1). K, J, or I step was positively correlated with the Mn level or the stress time in the Mn-treated leaves.

Positive L-band and K-band increased with the Mn levels on days 10, 25, and 40 (Fig. 2). In the L1-treated group, the L-band achieved the maximum value on day 10 and then decreased continuously to reach the control levels on day 40. In the L2-treated group, the maximum value of L-band appeared on day 25 and was maintained until day 40. The changes of K-band were similar to L-band except that the K-band in the L1-treated group on day 40 was higher than that of the controls.

Variable fluorescence at 2 ms (V_J) increased with the Mn levels (Table 2). There was no significant difference between the L1- or the L2-treated groups and control group except for the L2-treated group on day 40. A significant difference was observed between the L3- and L4-treated groups and the control group. Significant differences were also observed between the L4-treated group and the L1- or L2-treated groups. V_J was significantly higher on day 40 compared with day 10 in all Mn treatment levels. The variable fluorescence at 30 ms (V_I) increased with Mn levels (Table 2). V_I was significantly increased in L2-, L3- and L4-treated groups compared with the control group, while there was no significant difference between the L1-treated group and the control group. V_I was significantly increased in the L4-treated group compared with the L2-treated group on days 25 and day 40. There were no significant differences among the different stress time points.

Effects of Mn on the performance index, energy distribution, and the quantum yield of excitation energy trapping of PSII in *L. lucidum* leaves. We analyzed several functional parameters from the JIP-test to further characterize the effect of Mn on PSII of *L. lucidum*. Performance index (PI_{ABS}) showed a declining trend during the test period (Fig. 3a). PI_{ABS} in the L4-treated group was significantly decreased compared

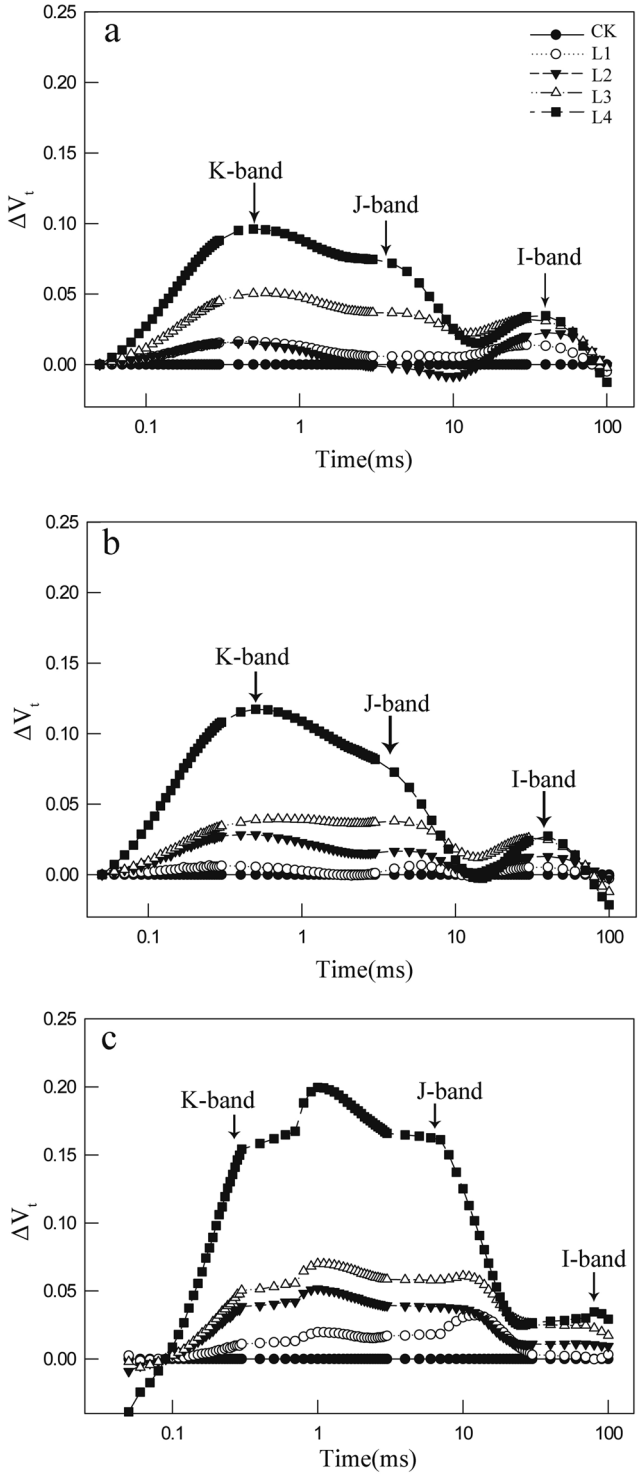

Figure 1. Changes in O-P phase relative variable fluorescence intensity (ΔV_t) in control group and four Mn-treated groups on day 10 (**a**), day 25 (**b**) and day 40 (**c**).

with the L1-treated group and the control group in a time-dependent manner. There was no significant difference between the L1- or L2-treated groups and the control group at any time point, except between the L2-treated group and the control group on day 40. In L3- and L4-treated groups, PI_{ABS} was significantly decreased on day 40 compared with day 10.

Absorption ABS/RC (Fig. 3b), trapping TR_o/RC (Fig. 3c), and dissipation DI_o/RC (Fig. 3e) were increased in a Mn-concentration dependent manner during the test period, and these parameters were significantly increased in the L4-treated group compared with the control group during the test period. No significant difference at the same levels of Mn was observed among various time points (day 10, 25 and 40). Electron transport ET_o/RC

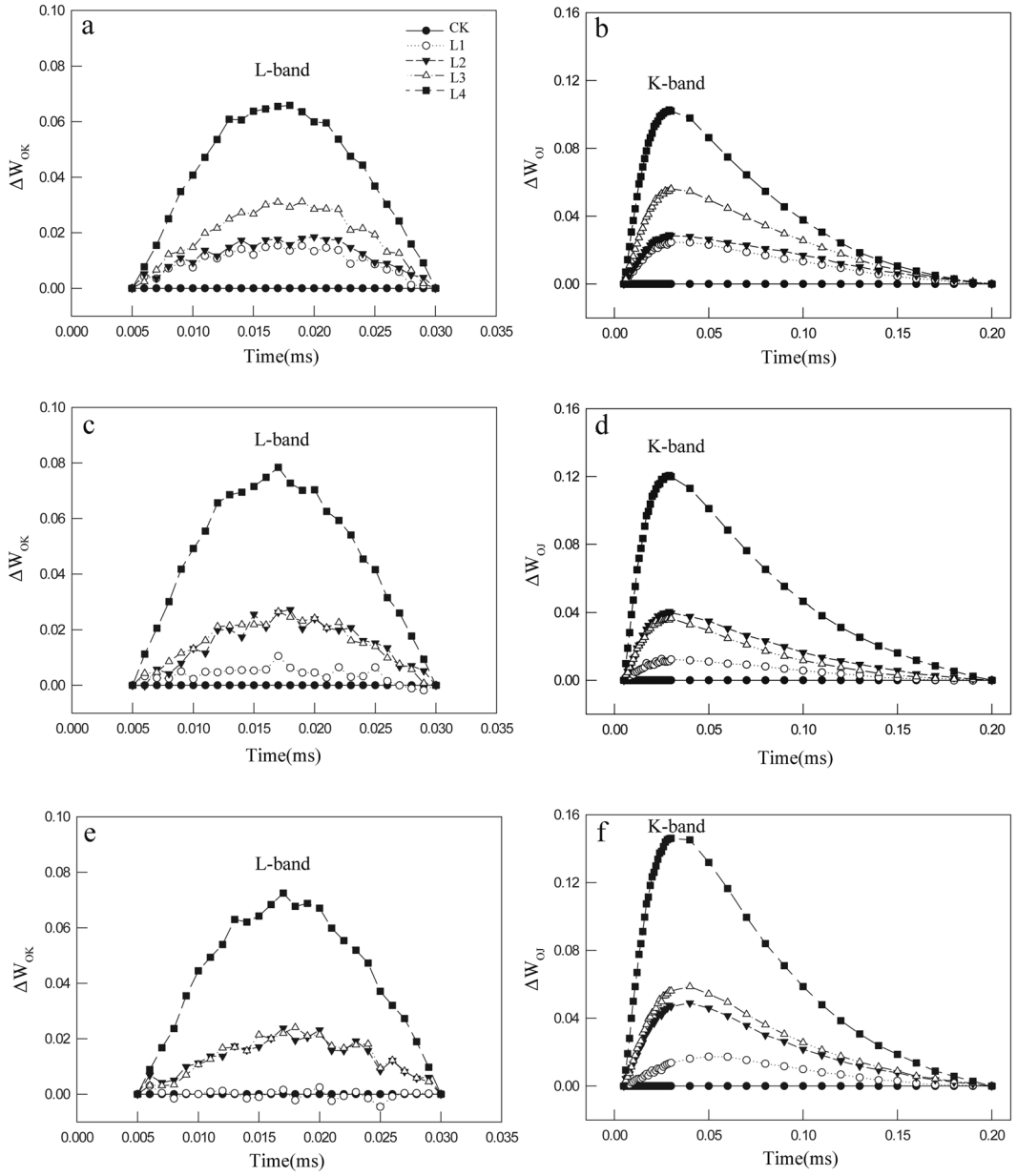

Figure 2. Changes in O-K phase relative variable fluorescence intensity (ΔW_{OK}, **a**–**c**), and in O-J phase relative variable fluorescence intensity (ΔW_{OJ}, **d**–**f**) in control group and four Mn-treated groups on day 10 (**a**,**d**), day 25 (**b**,**e**) and day 40 (**c**,**f**).

(Fig. 3d) first increased and then decreased along with the increase of Mn levels, and the maximum value of ET_o/RC was observed in the L2-treated group. There was no significant difference between the Mn-treated groups and control group at various time points, except between the L4-treated group and the control group on day 40.

Maximum quantum yield φ_{Po} (Fig. 3f), the probability that an absorbed photon moves an electron further than Q_A^- ($\varphi_{Eo}\psi_o$) (Fig. 3g), and the probability that a trapped exciton moves an electron further than Q_A^- (ψ_o) (Fig. 3h) at various time points showed a declining trend with increasing Mn levels. φ_{Po} was significantly decreased in the L4-treated group compared with the control on days 10, 25, and 40, and φ_{Po} was significantly decreased in L2, L3, and L4-treated groups compared with the control on day 40. φ_{Eo} and ψ_o were significantly decreased in the L2-, L3- and L4-treated groups compared with the control on day 40.

Interaction of stress time and Mn levels for Chl a fluorescence parameters (FPs) in *L. lucidum* leaves. All JIP-test parameters significantly varied with the Mn levels, and all parameters, except V_I, ABS/RC, TR_o/RC, DI_o/RC, and φ_{Po}, were significantly affected by the stress time. However, none of the parameters significantly responded to the interaction between Mn levels and stress time.

	Mn-treatment	Day 10	Day 25	Day 40
V_J	CK	0.530 ± 0.009 Aa	0.537 ± 0.010 Aa	0.542 ± 0.022 Aa
	L1	0.539 ± 0.005 ABa	0.538 ± 0.008 Aa	0.557 ± 0.004 ABb
	L2	0.534 ± 0.010 ABa	0.557 ± 0.014 Aab	0.588 ± 0.015 BCb
	L3	0.572 ± 0.009 Ba	0.576 ± 0.004 ABab	0.606 ± 0.005 Cb
	L4	0.614 ± 0.029 Ca	0.638 ± 0.045 Bab	0.720 ± 0.017 Db
V_I	CK	0.892 ± 0.005 Aa	0.896 ± 0.004 Aa	0.901 ± 0.004 Aa
	L1	0.905 ± 0.005ABa	0.902 ± 0.004 ABa	0.902 ± 0.004 ABa
	L2	0.912 ± 0.006 BCa	0.909 ± 0.004 BCa	0.913 ± 0.006 Ba
	L3	0.923 ± 0.005 Ca	0.922 ± 0.004 CDa	0.926 ± 0.001 Ca
	L4	0.926 ± 0.007 Ca	0.922 ± 0.003 Da	0.933 ± 0.002 Ca

Table 2. Fluorescence parameters (V_J and V_I) in the control and Mn-treated groups on day 10, day 25 and day 40. Values represent mean ± SE. Different capital letters represent significant difference between the different Mn-treatments in the same stress time points, and different lowercase letters represent significant difference between the same Mn- treatments in the different stress time points ($P < 0.05$). Mn-treatment = Manganese-treatment; CK = control; L1 = 12 mM manganese -treatment; L2 = 24 mM manganese -treatment; L3 = 36 mM manganese -treatment; L4 = 48 mM manganese -treatment; V_J = values of relative variable fluorescence at 2 ms; V_I = values of relative variable fluorescence at 30 ms.

	Mn level	Stress time	Mn level × Stress time
V_J	27.176**	10.695**	1.519
V_I	24.389**	1.396	0.427
PI_{ABS}	27.454**	5.753**	0.571
ABS/RC	14.637**	2.039	0.367
TR_0/RC	12.174**	1.802	0.279
ET_0/RC	3.879**	7.108**	0.921
DI_0/RC	17.893**	2.257	0.625
φ_{PO}	36.393**	0.065	0.204
φ_{EO}	31.667**	10.882**	1.515
ψ_0	27.176**	10.695**	1.519

Table 3. Two-way ANOVA results for JIP-test parameters. *$P < 0.05$, **$P < 0.01$. V_J = values of relative variable fluorescence at 2 ms; V_I = values of relative variable fluorescence at 30 ms; PI_{ABS} = Performance index (potential) for energy conservation from photons absorbed by PSII to the reduction of intersystem electron acceptors; ABS/RC = Absorption flux (of antenna Chls) per RC (also a measure of PSII apparent antenna size); TR_o/RC = Trapped energy flux (leading to Q_A reduction) per RC at t = 0; ET_o/RC = Electron transport flux (further than Q_A^-) per RC at t = 0; DI_o/RC = Dissipated energy flux per RC at t = 0; φ_{Po} = Maximum quantum yield for primary photochemistry; φ_{Eo} = Quantum yield for electron transport; ψ_o = Efficiency/probability that an electron moves further than Q_A^-.

Effects of Mn on net photosynthesis rate (Pn) and intercellular CO_2 concentration (C_i) in *L. lucidum* leaves. As reported in Table 4, Pn was significantly decreased in L2-, L3-, and L4-treated groups compared with the control. Further, Pn in the L3- and L4-treated groups was significantly decreased compared with the L1-treated group. C_i increased with the Mn levels (Table 4), but no significant differences were observed between the control and the Mn-treated groups.

Total contents of Mn in *L. lucidum* leaves, stems, and roots. The total Mn contents of plant organs were significantly higher in the Mn-treated *L. lucidum* than in the control except for the Mn levels in the leaves of the L1-treated group (Table 5). The Mn concentrations were highest in the roots, followed by the leaves, and the stems. The Mn content was significantly different among roots, stems, and leaves, except for between the stems and leaves in the L1-treated group.

Discussion

In this study, the OJIP curve was observed to be O-L-K-J-I-P when the Mn levels increased (Figs 1 and 2). The OJIP curve is very sensitive to environmental stress[16,21,24]. In leaves that have been exposed to a disturbed environment for a short period of time, Chl a fluorescence shows a polyphasic rise before J step, and the O-J-I-P becomes O-K-J-I-P and even O-L-K-J-I-P[16,26].

The L-band (~150 μs) is an indicator of energetic connectivity of the antennae to PSII units[24,27], implying better excitation energy utilization and system stability of PSII units[21,27]. In our study, the presence of positive L-band in the Mn-treated leaves indicated an inferior performance of antennae connectivity compared to the control leaves and might be a sign of disturbed energy transfer[28]. According to the Grouping Concept and JIP-test[21,26], the

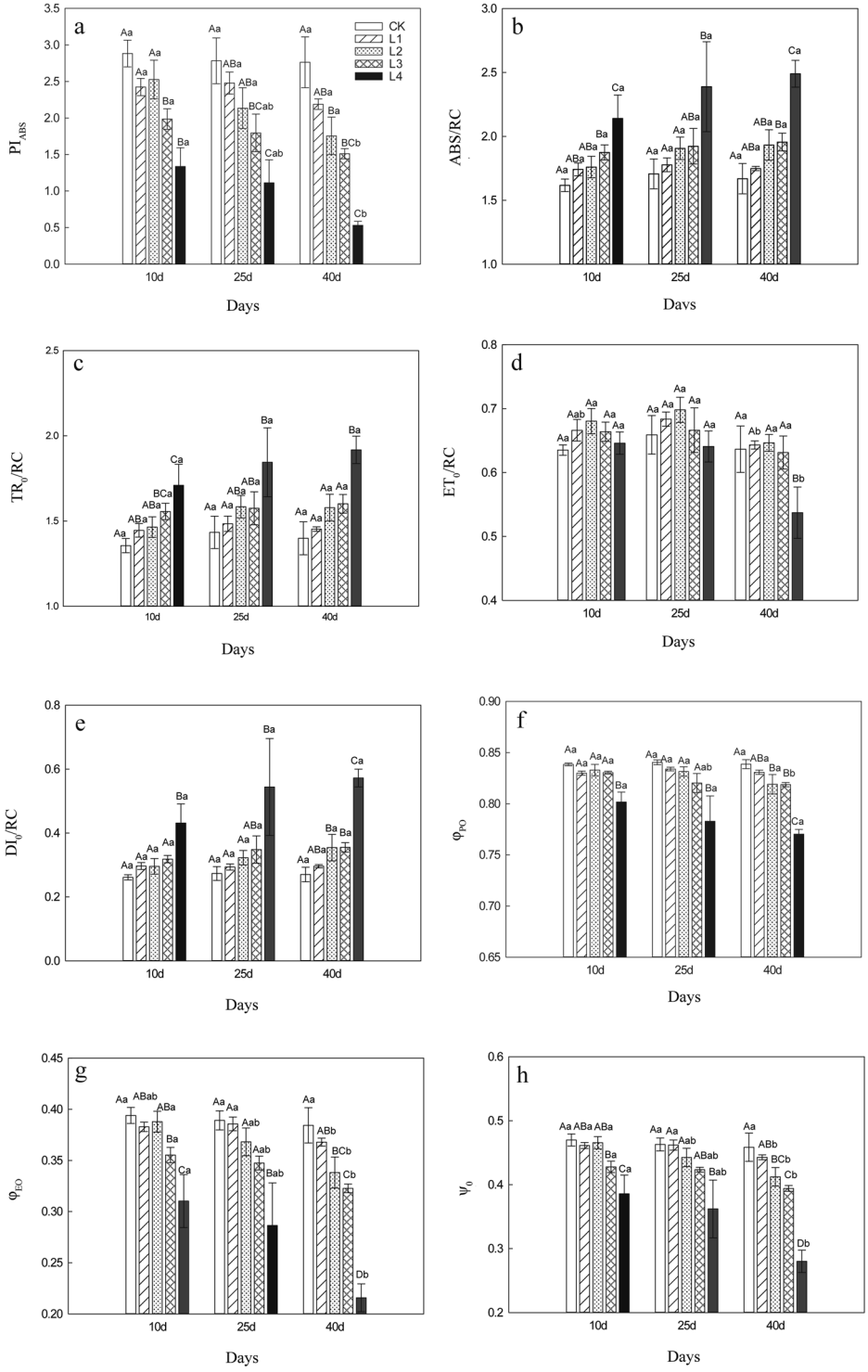

Figure 3. Mn induced changes in performance index (PI_{ABS}, **a**), absorption (ABS/RC, **b**), trapping (TR_o/RC, **c**), electron transport (ET_o/RC, **d**), dissipation (DI_o/RC, **e**), the maximum quantum yield of primary photochemistry (φ_{Po}, **f**), the quantum yield of electron transport (φ_{Eo}, **g**) and the efficiency (ψ_o, **h**). Values represent mean ± SE. Different capital letters represent significant difference between the different Mn-treatments in the same stress time points, and different lowercase letters represent significant difference between the same Mn- treatments in the different stress time points ($P < 0.05$).

positive L-band implies that the PSII units were less tightly grouped, or that less energy was exchanged between the independent PSII units. Therefore, PSII units of Mn-treated leaves had lower stability and became more fragile. However, an amplitude change in the L-band (from positive to negative) of the L1-treated group was observed

Mn-treatment	Ck	L1	L2	L3	L4
Pn	5.330 ± 0.337 A	4.563 ± 0.777 AB	3.364 ± 0.492 BC	2.419 ± 0.459 C	1.922 ± 0.289 C
Ci	145.741 ± 12.414 A	154.09 ± 7.245 A	159.422 ± 15.331 A	164.086 ± 22.819 A	193.997 ± 0.043 A

Table 4. Net photosynthesis rate (Pn, $\mu molCO_2 \cdot m^{-2} \cdot s^{-1}$) and intercellular CO_2 concentration (Ci, $\mu mol\ mol^{-1}$) in the control and Mn-treated groups on day 40. Values represent mean ± SE. Different capital letters represent significant difference among Mn-treatments ($P < 0.05$). Mn-treatment = Manganese-treatment; Pn = net photosynthesis rate; CK = control; L1 = 12 mM manganese-treatment; L2 = 24 mM manganese -treatment; L3 = 36 mM manganese -treatment; L4 = 48 mM manganese–treatment.

	Mn (mg/kg DW)		
Mn-treatment	roots	stems	leaves
Ck	168.09 ± 17.15Aa	74.92 ± 0.61Ab	192.85 ± 6.88Aa
L1	1576.16 ± 32.01Ba	827.22 ± 17.48Bb	1014.11 ± 202.98Ab
L2	2427.31 ± 15.60Ba	1015.68 ± 47.06BCb	2069.53 ± 46.66Bc
L3	5183.54 ± 258.48Ca	1186.83 ± 68.92Cb	2788.06 ± 480.70Bc
L4	10990.59 ± 668.02Da	1608.17 ± 121.03Db	5108.64 ± 364.31Cc

Table 5. Mn content in roots, stems and leaves on day 40. Values represent mean ± SE. Different capital letters represent significant difference among Mn-treatments ($P < 0.05$), different lowercase letters represent significant difference in the different plant organs between the same Mn- treatments ($P < 0.05$). Mn-treatment = Manganese-treatment; DW = dry weight; CK = control; L1 = 12 mM manganese-treatment; L2 = 24 mM manganese -treatment; L3 = 36 mM manganese -treatment; L4 = 48 mM manganese-treatment.

from day 10 to day 40 (Fig. 2a,c,e) suggesting that the PSII units had better excitation energy utilization and system stability on day 40 without any irreversible damage. This may be associated with a lack of significant Mn accumulation in the leaves of the L1-treated groups (compared to controls, Table 5).

The K-band can be explained by the imbalance of electron flow from the donor side to the acceptor side in the PSII RCs[28]. When the electron transfer from the OEC to tyrosine Z (Y_z) is slower than the electron transfer from P680 to Q_A and beyond, there is a high accumulation of Y_z^+[25]. Thus, this accumulation of Y_z^+ causes the appearance of K-step, which is directly associated with an inactivation of the OEC[25]. In this study, the appearance of K step suggested that Mn inhibit the electron flow from the donor to the acceptor side of PSII even at low levels (L1) (Fig. 1a–c). Meanwhile, the presence of positive K-band in the Mn-treated leaves indicates an inactivation of the OEC[24,25] (Fig. 2d–f). Therefore, it may be inferred that the competition between Ca^{2+} and Mn^{2+}[29] in the OEC led to more sites held by Mn^{2+} in the OEC, and this may depend on the similar ion radius and charge properties of Mn^{2+} and Ca^{2+}[30].

OJIP transients can be used to examine the electron transport flux from PSII RCs to PSI through Q_A and Q_B. In this study, leaves in the L3- and L4-treated groups had significantly increased V_J compared with the control leaves (Table 2), indicating that high levels of Mn induced the accumulation of Q_A^-. This result is consistent with the previous findings[16,26,27]. The increased value of V_J could be related to the blockade of electron transport downstream of Q_A by Mn stress[31]. This finding is also supported by the decrease of φ_{Eo} and ψ_o (Fig. 3g,h), as Q_B was unable to be reduced by Q_B-non-reducing PSII RCs[27,32]. Correspondingly, the higher levels of Q_B-non-reducing centers blocked electron transport towards PSI[32]. Lower redox state of Q_B implies altered reduction potential of PSII at the acceptor side in Mn-stressed plants[17]. Since Q_A is in quasi-equilibrium with Q_B and the PQ pool, the lower redox potential of Q_B will decrease the probability of forward electron transfer between the two quinone acceptors by shifting the redox equilibrium between $Q_A^-Q_B$ and $Q_AQ_B^-$ towards $Q_A^-Q_B$[33,34].

The significant reduction of PI_{ABS}, which is a very sensitive indicator of plant functionality[27], indicates that excessive Mn may down-regulate PSII function, resulting in prolonged negative effect with irreversible damage. An increase in both ABS/RC and TR_o/RC, and a decrease in φ_{Po} indicates inactivation of a certain part of RCs, which was most likely due to inactivation of OEC as well as the transformation of active RCs to silent ones, because the functional antenna that supplies excitation energy to active RCs was increased in size[24,27]. However, an increase in ET_o/RC under low levels of Mn (L1 and L2) implies that these inactive RCs[35] could prevent further damage to themselves and protect neighboring active RCs in response to the absorbed light energy in the active RCs[36]. Significantly increased DI_o/RC and decreased ET_o/RC in the highest Mn treatment group (L4) shows that the excess excitation energy was mostly dissipated[21,24].

ANOVA results revealed that all JIP-test parameters used in this study were significantly affected by Mn stress ($P < 0.05$), but the interactive influences of Mn stress and stress time on the examined parameters were not significant ($P > 0.05$) (Table 3). We also found that *L. lucidum* leaves were more sensitive to the Mn levels compared with the stress time. Additionally, ET_o/RC, φ_{Eo}, and ψ_o were significantly influenced by Mn stress time, indicating that the blockage of PSII electron flow beyond Q_A^- was more severe in response to the increasing stress time. The blockage of PSII electron flow was also supported by the phenomena of the accumulation of Q_A^- and the increase in V_J.

The Mn-induced changes in the shape of OJIP transient curves and other related parameters of *L. lucidum* as observed in this study were also found in the studies of Mn-treated *Citrus grandis* seedlings[16], Al-treated

Citrus grandis[26], and Cd-treated *Solanum lycopersicum*[37]. But different from our results here, Cr-treated *Spirodela polyrhiza* was found to have a decreasing trend of TR_o/RC, indicating that the Cr damages LHCs[38]. Therefore, the sensitivity of different parts of the PSII units vary, and this response is the different for different heavy metals and is species-dependent.

This study found that Pn of the plants in L2, L3 and L4 treatments was significantly lower than that in the control (Table 4), and Pn and Ci were negatively correlated. Therefore the reduced Pn observed in our study was not caused by Ci limitation[39,40]. A negative correlation between Ci and Pn was suggested as an indicator to describe the decrease in carboxylation efficiency by Rouhi *et al.*[41]. A positive relationship between maximum quantum yield of PSII (Fv/Fm) and Pn was also found by Tezara *et al.*[42]. These results suggested that the reduction of Pn could be explained by the limitation in photochemical activity of PSII, which impeded the utilization of CO_2 in the assimilation process. The current study found that excessive Mn impaired the functional PSII, as supported by the observed positive L-band and the observed decrease in PI_{ABS}. Thus, Mn toxicity contributed to the observed significant reduction of Pn through its effects on photosynthetic apparatus[43].

Conclusions

We conclude that an excess level of Mn affected the net photosynthesis rate, the OJIP transient, and other related parameters of *L. lucidum* seedlings. The imaging of JIP-Test parameters revealed Mn-induced photo-damage on the PSII RCs, including a decrease in energy absorption and excitation energy trapping, and an increase in energy dissipation. The disturbance of the PSII electron transport from the donor side to the acceptor side might be associated with inactivation of OEC. This, in turn, resulted in a decrease in the rate of electron transport beyond Q_A and an accumulation of Q_A^-.

References

1. Matile, P. H., Hortensteiner, S., Thomas, H. & Krautler, B. Chlorophyll breakdown in senescent leaves. *Plant Physiol* **112**, 1403–1409 (1996).
2. Bernhard, K., Warren, M. J. & Smith, A. G. *Chlorophyll breakdown[M]//Tetrapyrroles*. (Springer, New York, 1970).
3. Paul, S., Neese, F. & Pantazis, D. A. Structural models of the biological oxygen-evolving complex: achievements, insights, and challenges for biomimicry. *Green Chem* **19**, 2309–2325 (2017).
4. Millaleo, R., Reyes-Díaz, M., Ivanov, A. G., Mora, M. L. & Alberdi, M. Manganese as essential and toxic element for plants: transport, accumulation and resistance mechanisms. *J Soil Sci Plant Nut* **10**, 476–494 (2010).
5. Ning, D., Wang, F., Zhou, C. B., Zhu, C. L. & Yu, H. B. Analysis of pollution materials generated from electrolytic manganese industries in china. *Resour Conserv Recy* **54**, 506–511 (2010).
6. Javed, M. & Usmani, N. Assessment of heavy metal (Cu, Ni, Fe, Co, Mn, Cr, Zn) pollution in effluent dominated rivulet water and their effect on glycogen metabolism and histology of Mastacembelus armatus. *SpringerPlus* **2**, 390 (2013).
7. Demirezen, D. & Aksoy, A. Common hydrophytes as bioindicators of iron and manganese pollutions. *Ecol Indic* **6**, 388–393 (2006).
8. Wang, X. *et al*. Pedological characteristics of Mn mine tailings and metal accumulation by native plants. *Chemosphere* **72**, 1260–1266 (2008).
9. Rayen, M., Reyes-Díaz, M., Ivanov, A. G., Mora, M. L. & Alberdi, M. Manganese as essential and toxic element for plants: transport, accumulation and resistance mechanisms. *J Soil Sci Plant Nut* **10**, 476–494 (2010).
10. Führs, H. *et al*. Physiological and proteomic characterization of manganese sensitivity and tolerance in rice (Oryza sativa) in comparison with barley (Hordeum vulgare). *Ann Bot* **105**, 1129–1140 (2010).
11. Nable, R. O., Houtz, R. L. & Cheniae, G. M. Early inhibition of photosynthesis during development of Mn toxicity in tobacco. *Plant Physiol* **86**, 1136–1142 (1988).
12. González, A. & Lynch, J. P. Subcellular and tissue Mn compartmentation in bean leaves under Mn toxicity stress. *Aust J Plant Physiol* **26**, 811–822 (1999).
13. Feng, J. P., Shi, Q. H. & Wang, X. F. Effects of exogenous silicon on photosynthetic capacity and antioxidant enzyme activities in chloroplast of cucumber seedlings under excess manganese. *J Integr Agr* **8**, 40–50 (in Chinese) (2009).
14. González, A. & Lynch, J. P. Effects of manganese toxicity on leaf CO2, assimilation of contrasting common bean genotypes. *Physiol Plantarum* **101**, 872–880 (1997).
15. Kitao, M., Lei, T. T. & Koike, T. Comparison of photosynthetic responses to manganese toxicity of deciduous broad-leaved trees in northern Japan. *Environ Pollut* **97**, 113–118 (1997).
16. Li, Q. *et al*. Effects of manganese-excess on CO2, assimilation, ribulose-1,5- bisphosphate carboxylase/oxygenase, carbohydrates and photosynthetic electron transport of leaves, and antioxidant systems of leaves and roots in Citrus grandis seedlings. *BMC Plant Biol* **10**, 1–16 (2010).
17. Doncheva, S. *et al*. Silicon amelioration of manganese toxicity in Mn-sensitive and Mn-tolerant maize varieties. *Environ Exp Bot* **65**, 189–197 (2009).
18. Subrahmanyam, D. & Rathore, V. S. Influence of manganese Toxicity on photosynthesis in Ricebean (Vigna umbellata) Seedlings. *Photosynthetica* **38**, 449–453 (2001).
19. Kitao, M., Lei, T. T. & Koike, T. Effects of manganese toxicity on photosynthesis of white birch (Betula platyphylla var. japonica) seedlings. *Physiol Plantarum* **101**, 249–256 (1997).
20. Magyar, M. *et al*. Rate-limiting steps in the dark-to-light transition of Photosystem II - revealed by chlorophyll-a fluorescence induction. *Sci Rep* 8–2755 (2018).
21. Strasser, R. J., Tsimilli-michael, M. & Srivastava, A. Analysis of the chlorophyll a fluorescence. In *Chlorophyll a Fluorescence: A Signature of Photosynthesis* (eds Papageorgiou, G. C. & Govindjee) 463–495 (Springer, 2004).
22. Trikshiqi, R. & Rexha, M. Heavy metal monitoring by *Ligustrum lucidum*, Fam: Oleaceae vascular plant as bio-indicator in Durres city. *Int J Curr Res* **7**, 14415–14422 (2015).
23. He, Z. X., Zhu, F. & Chen, Y. H. Distribution and pollution evaluation of heavy metals in mine soils of Chang-Zhu-Tan city region. *J C S Univ For Tech*. **31**, 196–199 (in Chinese) (2011).
24. Yusuf, M. A. *et al*. Overexpression of γ-tocopherol methyl transferase gene in transgenic Brassica juncea plants alleviates abiotic stress: physiological and chlorophyll a fluorescence measurements. *BBA-Bioenergetics* **1797**, 1428–1438 (2010).
25. Strasser, B. J. Donor side capacity of photosystem II probed by chlorophyll a fluorescence transients. *Photosynth Res* **52**, 147–155 (1997).
26. Jiang, H. X. *et al*. Aluminum-induced effects on photosystem II photochemistry in Citrus leaves assessed by the chlorophyll a fluorescence transient. *Tree Physiol* **28**, 1863–1871 (2008).
27. Mlinarić, S., Dunić, J. A., Babojelić, M. S., Cesar, V. & Lepeduš, H. Differential accumulation of photosynthetic proteins regulates diurnal photochemical adjustments of PSII in common fig (Ficus carica L.) leaves. *J Plant Physiol* **209**, 1–10 (2017).

28. Srivastava, A., Guissé, B., Greppin, H. & Strasser, R. J. Regulation of antenna structure and electron transport in Photosystem II of Pisum sativum, under elevated temperature probed by the fast polyphasic chlorophyll a, fluorescence transient: OKJIP. *BBA Bioenergetics* **1320**, 95–106 (1997).
29. Dasgupta, J., Ananyev, G. M. & Dismukes, G. C. Photoassembly of the water-oxidizing complex in photosystem II. *Coordin Chem Rev* **252**, 347–360 (2008).
30. Chao, S. H., Suzuki, Y., Zysk, J. R. & Cheung, W. Y. Activation of calmodulin by various metal cations as a function of ionic radius. *Mol Pharmacol* **26**, 75–82 (1984).
31. Schansker, G. & Strasser, R. J. Quantification of non-QB-reducing centers in leaves using a far-red pre-illumination. *Photosynth Res* **84**, 145–151 (2005).
32. Jiang, C. D., Jiang, G. M., Wang, X. & Li, Y. G. Increased photosynthetic activities and thermostability of photosystem II with leaf development of elm seedlings (Ulmus pumila) probed by the fast fluorescence rise OJIP. *Environ Exp Bot* **58**, 261–268 (2006).
33. Minagawa, J., Narusaka, Y., Inoue, Y. & Satoh, K. Electron transfer between QA and QB in photosystem II is thermodynamically perturbed in phototolerant mutants of Synechocystis sp. PCC 6803. *Biochemistry* **38**, 770–775 (1999).
34. Ivanov, A. G., Sane, P. V., Zeinalov, Y. & Oquist, G. Seasonal responses of photosynthetic electron transport in Scots pine (Pinus sylvestris L.) studied by thermoluminescence. *Planta* **215**, 457–465 (2002).
35. Singh, S. & Prasad, S. M. IAA alleviates Cd toxicity on growth, photosynthesis and oxidative damages in eggplant seedlings. *Plant Growth Regul* **77**, 87–98 (2015).
36. Samuelsson, G. & Richardson, K. Photoinhibition at low quantum flux densities in a marine dinoflagellate (Amphidinium carterae). *Mar Bio* **70**, 21–26 (1982).
37. Singh, S. & Prasad, S. M. Effects of 28-homobrassinoloid on key physiological attributes of Solanum lycopersicum seedlings under cadmium stress: Photosynthesis and nitrogen metabolism. *Plant Growth Regul* **82**, 1–13 (2017).
38. Appenroth, K. J., Stöckel, J., Srivastava, A. & Strasser, R. J. Multiple effects of chromate on the photosynthetic apparatus of Spirodela polyrhiza as probed by OJIP chlorophyll a fluorescence measurements. *Environ Pollut* **115**, 49–64 (2001).
39. Li, Y. *et al*. Effect of combined pollution of Cd and B[a]P on photosynthesis and chlorophyll fluorescence characteristics of wheat. *Pol J Environ Stud* **24**, 157–163 (2015).
40. Chu, J. J. *et al*. Effects of cadmium on photosynthesis of Schima superba young plant detected by chlorophyll fluorescence[J]. *Environ Sci Pollut R* **25**, 1–9 (2018).
41. Rouchi, V., Samson, R., Lemeur, R. & Van Damme, P. Photosynthetic gas exchange characteristics in three different almond species during drought stress and subsequent recovery. *Environ Exp Bot* **59**, 117–129 (2007).
42. Tezara, W., Marin, O., Rengifo, E., Martinez, D. & Herrera, A. Photosynthesis and photo-inhibition in two xerophytic shrubs during drought. *Photosynthetica* **43**, 37–45 (2005).
43. Mohapatra, P. K., Khillar, R., Hansdah, B. & Mohanty, R. C. Photosynthetic and fluorescence responses of Solanum melangena L. to field application of dimethoate. *Ecotox Environ Safe* **73**, 78–83 (2010).

Acknowledgements

The authors thank Key Research and Development Project of Hunan Province (2017NK2171), "948" introduction project of The State Bureaucracy of Forestry (2014-4-62) and Nature Science Foundation of Hunan Provincial Innovative Research Team (2013) for financial support. We thanks Dr. S.G. Liu and D.Y. Fan for stimulating discussions and critical readings of the manuscript.

Author Contributions

H.Z.L. and F.Z. designed the research and wrote the main manuscript, H.Z.L., R.J.W. and X.H.H. conducted the experiment, R.J.W., X.H.H. and J.J.C. analyzed data. All authors reviewed the manuscript.

Additional Information

Competing Interests: The authors declare no competing interests.

Publisher's note: Springer Nature remains neutral with regard to jurisdictional claims in published maps and institutional affiliations.